Regional Coherence Evaluation in Mild Cognitive Impairment and Alzheimer's Disease Based on Adaptively Extracted Magnetoencephalogram Rhythms

Javier Escudero[1,2,3], Saeid Sanei[2,4], Delaram Jarchi[2], Daniel Abásolo[3,5] and Roberto Hornero[3]

[1]Signal Processing and Multimedia Communication, School of Computing and Mathematics, University of Plymouth, Drake Circus, Plymouth, PL4 8AA, UK.
[2]Centre of Digital Signal Processing, Cardiff University, Cardiff, CF24 3AA, UK.
[3]Biomedical Engineering Group, University of Valladolid, Valladolid, 47011, Spain.
[4]Faculty of Electronic Engineering, Physics and Computing, University of Surrey, Guildford, GU2 7XH, UK.
[5]Centre for Biomedical Engineering, Division of Mechanical, Medical & Aerospace Engineering, University of Surrey, Guildford, GU2 7XH, UK.

E-mail: `javier.escudero@ieee.org`

E-mail: `javier.escudero@plymouth.ac.uk`

Abstract. This study assesses the connectivity alterations caused by Alzheimer's disease (AD) and mild cognitive impairment (MCI) in the magnetoencephalogram (MEG) background activity. Moreover, a novel methodology to adaptively extract brain rhythms from the MEG is introduced. This methodology relies on the ability of an Empirical Mode Decomposition (EMD) to isolate local signal oscillations and a constrained Blind Source Separation (cBSS) to extract the activity that jointly represents a subset of channels. Inter-regional MEG connectivity was analysed for 36 AD, 18 MCI, and 26 control subjects in δ, θ, α, and β bands over left and right central, anterior, lateral, and posterior regions with magnitude squared coherence – $c(f)$. For the sake of comparison, $c(f)$ was calculated from the original MEG channels and from the adaptively extracted rhythms. The results indicated that AD and MCI cause slight alterations in the MEG connectivity. $c(f)$ computed from the extracted rhythms distinguished AD and MCI subjects from controls with 69.4% and 77.3% accuracies, respectively, in a full leave-one-out cross-validation evaluation. These values were higher than those obtained without the proposed extraction methodology.

PACS numbers: 87.85.Ng, 87.19.le, 87.19.xr

Keywords: Alzheimer's Disease (AD), Magnitude Squared Coherence – $c(f)$, Constrained Blind Source Separation (cBSS), Empirical Mode Decomposition (EMD), Magnetoencephalogram (MEG), Mild Cognitive Impairment (MCI)

Submitted to: *Physiol. Meas.*

1. Introduction

Alzheimer's Disease (AD) is a neurodegenerative disorder. It causes memory loss and other cognitive and behavioural symptoms that progressively impair the daily activities (Blennow et al., 2006; Nestor et al., 2004). AD is the most common form of dementia in the western world. It accounts for 50% to 60% of all dementia cases (Blennow et al., 2006). Its prevalence increases almost exponentially with age (Blennow et al., 2006; Nestor et al., 2004). As a consequence, AD is one of the most disabling and burdensome health conditions worldwide (Ferri et al., 2006). A definite diagnosis of AD can only be made by necropsy (Blennow et al., 2006). In clinical practice, AD is diagnosed based on the criteria set by McKhann et al. (1984). Yet, the accuracy is limited (Blennow et al., 2006). Hence, it is important to develop methods to help in AD diagnosis in order to improve the patients' care and allow more accurately targeted future therapies.

Mild Cognitive Impairment (MCI) shares some features with AD. The cognitive deficits of MCI subjects are limited to memory but their activities of daily living are preserved (Nestor et al., 2004). Thus, this concept could represent a transitional period before full-blown dementia (Blennow et al., 2006; Nestor et al., 2004). The rate of conversion to AD is about ten times higher for MCI subjects than that for the general population. Yet, the narrow definition of MCI might fail to capture the heterogeneity of clinical AD (Nestor et al., 2004).

Spectral (Abatzoglou et al., 2009; Escudero et al., 2009; Poza et al., 2008; Rossini et al., 2007) and non-linear analysis techniques (Abásolo et al., 2008; Abatzoglou et al., 2007; Gómez et al., 2009a; van Cappellen van Walsum et al., 2003) have been applied to single channels of electroencephalogram (EEG) and magnetoencephalogram (MEG) recordings from AD patients. The general conclusion of those studies is that AD causes both a spectral slowdown and alterations in the non-linear dynamics of the electromagnetic brain activity (Hornero et al., 2009; Jeong, 2004; Stam, 2010). Additionally, AD can be characterised as a disconnection syndrome (Jeong, 2004; Stam et al., 2006, 2009). The brain activity has also been studied in MCI subjects (Babiloni et al., 2006; Fernández et al., 2006; Rossini et al., 2006, 2008). Overall, differences are more easily found between healthy elderly subjects and AD patients than for MCI subjects (Jeong, 2004; Stam, 2010). This may be due to the small gap between the MCI subjects and the other two groups (Fernández et al., 2006; Gómez et al., 2009b). Given that MCI is considered as an intermediate state between healthy ageing and full-blown AD, MCI subjects might also show connectivity alterations in their brain recordings (Gómez et al., 2009b). The connectivity of the electromagnetic brain activity might help to predict the development of AD in MCI subjects (Rossini et al., 2006). Moreover, MEG has some desirable properties over the EEG when studying brain activity. MEG recordings are reference-free and less affected by extra-cerebral tissues than EEG signals (Rossini et al., 2007; Stam, 2010).

Magnitude Squared Coherence – $c(f)$ – is a widespread connectivity metric, which provides a measure of the linear dependencies between two signals as a function of frequency (Dauwels et al., 2010; Pereda et al., 2005). It has been hypothesised that AD decreases $c(f)$ in α and β but there are no conclusive findings about the δ and θ bands (Jeong, 2004; Rossini et al., 2007). Furthermore, AD produces opposite changes in features computed from different spectral bands (Alonso et al., 2011; Stam et al., 2009; van Cappellen van Walsum et al., 2003). Thus, it is advisable to analyse different spectral bands separately (Stam, 2010).

Yet, $c(f)$ has several limitations. Firstly, spurious correlations could appear due to the volume conduction (Gómez et al., 2009b; Nolte et al., 2004; Stam et al., 2009). This effect is due to the fact that nearby channels are likely to record activity from identical currents. This leads to abnormally high correlations in the results that reflect volume conduction rather than actual connectivity (Gómez et al., 2009b; Nolte et al., 2004; Stam et al., 2009). Other alternatives, such as the imaginary part of the coherency (Nolte et al., 2004) or the phase lag index (Stam et al., 2009), have been proposed. However, their use is much more limited and their interpretation is less straightforward than for $c(f)$ (Nolte et al., 2004; Stam et al., 2009). Furthermore, these measures are usually applied in a channel-wise manner, producing a very high number of variables (Dauwels et al., 2010; Gómez et al., 2009b). A possible option is to try to estimate the equivalent current dipoles (Hoechstetter et al., 2004; Rossini et al., 2007; Supp et al., 2007). Once the currents have been estimated, the same connectivity metrics used in the channel-wise analyses can be applied to them. Moreover, the volume conduction effect does not affect these dipole-based connectivity assessments (Hoechstetter et al., 2004; Supp et al., 2007). However, the solution of the inverse problem is not unique and the choice of the reconstruction algorithm and other a priori assumptions influence the estimation of the dipoles resulting in potentially misleading results (Nolte et al., 2004; Stam, 2010; Stam et al., 2006).

As an alternative to those two approaches, we apply $c(f)$ to groups of channels to characterise MEG background activity in AD and MCI. We want to study the spontaneous MEG in MCI and AD patients in contrast to elderly controls. $c(f)$ is computed from pairs of channels and the results are grouped attending at the location of channels over the scalp to estimate inter-regional coherence, likewise Stam et al. (2006). Our results complement the intra-regional connectivity analysis by Alonso et al. (2011), who analysed a smaller set of AD and control subjects by computing $c(f)$ and mutual information between pairs of channels in the same region. Their results suggested that AD is characterised by both decreases and increases of intra-regional connectivity in different frequency bands (Alonso et al., 2011). We also introduce a novel methodology to extract the activity that simultaneously represents a group of channels. It relies on the adaptiveness of the Empirical Mode Decomposition (EMD) (Huang et al., 1998) and the ability of a constrained Blind Source Separation (cBSS) (Lu and Rajapakse, 2005) to extract brain activity. We hypothesise that this novel procedure could compute an adaptive regional extraction of signals with useful information about the brain activity. Actually, the EMD and cBSS have already been combined by Ye-Lin et al. (2010) to denoise electroenterogram recordings. Their results support the usefulness of combining adaptive signal processing methodologies like EMD and Blind Source Separation (BSS).

2. Subjects and MEG recordings

MEG signals were acquired from 80 subjects: 36 AD, 18 MCI and 26 control subjects. Clinical diagnosis was ascertained with exhaustive medical, neurological, psychiatric, neuroimaging (SPECT and MRI), and neuropsychological examinations. The Mini-Mental State Examination (MMSE) (Folstein et al., 1975) and the Global Deterioration Scale/Functional Assessment Staging (GDS/FAST) (Reisberg, 1988) were used to screen the cognitive and functional status, respectively. All controls and patients' caregivers gave informed consent for participation in the study, which was approved by the local Ethics Committee.

The 36 AD patients (12 males and 24 females) fulfilled the criteria for probable AD according to the guidelines of the National Institute of Neurological of Communicative Disorders and Stroke – AD and Related Disorders Association (NINCDS–ADRDA) (McKhann et al., 1984). Their mean age was 74.06 ± 6.95 years (mean ± standard deviation, SD) and the average scores in the cognitive and functional tests were 18.06 ± 3.36 for MMSE, and 4.17 ± 0.45 for GDS/FAST (mean ± SD).

The MCI group was formed by 18 subjects (8 males and 10 females; age = 74.89 ± 5.57 years, mean ± SD) diagnosed following the Petersen's criteria (Petersen et al., 2001). Two of them were categorised as amnesic MCI, while the others were included in the multiple-domain category. The MCI patients' MMSE score was 25.67 ± 1.81 (mean ± SD) and all of them scored three in the GDS/FAST test.

Finally, 26 elderly control subjects (9 males and 17 females; age = 71.77 ± 6.38 years, mean ± SD) also participated in this study. The MMSE and GDS/FAST scores for the control group were 28.88 ± 1.18 and 1.73 ± 0.45 (mean ± SD), respectively. The difference in the mean age of the groups (both pair-wise and when all three groups were simultaneously considered) was not statistically significant (in all cases $p > 0.10$, Student's t-test). Patients and control subjects were free of significant neurologic and psychiatric diseases other than AD or MCI. None of them was taking medication that could affect the MEG activity.

The MEG recordings were acquired using a 148-channel whole-head magnetometer (MAGNES 2500 WH, 4D Neuroimaging) located in a magnetically shielded room at the "Centro de Magnetoencefalografía Dr. Pérez-Modrego," Spain. The MEGs were recorded whilst the subjects lay on a hospital bed in a relaxed state, awake, and with eyes closed. For each subject, five minutes of MEG background activity were recorded at 678.19 Hz with a 0.1–200 Hz hardware bandpass filter. The MEG equipment decimated each 5-minute dataset by a factor of four as a trade-off between data length reduction and accurate representation of the δ, θ, α and β bands. This process consisted of filtering the data to avoid aliasing and downsampling the recordings. This anti-aliasing filter was a second-order Butterworth IIR filter with cut-off frequency at 76.30 Hz (45% of the final sample rate: 169.55 Hz), which was applied to the signals in both forward and reverse directions to avoid net phase shift. Per subject, 17.25 ± 6.47 (mean ± SD) epochs of 10 s (1695 samples) with minimal ocular activity were visually selected for analysis by an expert unaware of the subjects' clinical situation with the aid of an amplitude thresholding method (Hornero et al., 2008).

Finally, in order to avoid biasing the computation of $c(f)$, the cardiac artefact was removed from the recordings with a cBSS-based procedure since this artefact can seriously affect the MEGs (Dammers et al., 2008; Escudero et al., 2007, 2011; James and Gibson, 2003). We used the average of all MEG channels as a reference of the cardiac activity in each epoch (Escudero et al., 2011). This average of all channels emphasises the cardiac artefact whereas the MEG background activity tends to cancel out as the cardiac artefact affects all channels simultaneously (Escudero et al., 2007, 2011). Thus, the cardiac artefact could be enhanced in the average of the MEG channels (Escudero et al., 2007, 2011). Then, an ECG-like template was derived from this average to guide a cBSS-based artefact removal (Escudero et al., 2011). For the interested reader, alternative BSS-based procedures to remove the cardiac activity are also available elsewhere. For instance, Sander et al. (2007) combined spectral, topographical, and temporal features to identify the cardiac activity, while Dammers et al. (2008) relied on amplitude and phase statistics to recognise and remove this artefact. Some cardiac artefact removal methods have been compared by Escudero

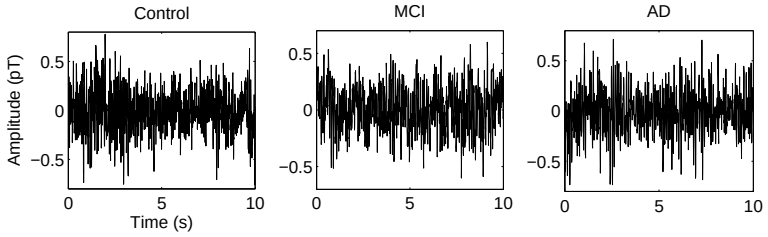

Figure 1: MEG signals recorded at channel 62, which is located in the right posterior region, for a control, MCI subject and AD patient. Amplitude and time are given in picoTesla (pT) and second (s) units, respectively.

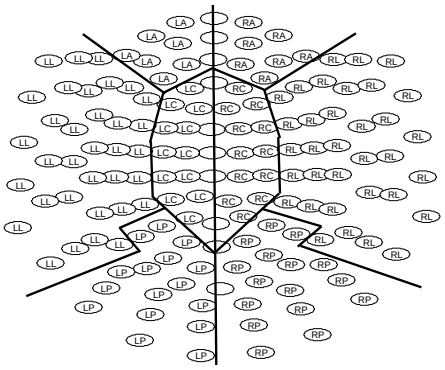

Figure 2: Distribution of the MEG sensors into Left Central (LC), Anterior (LA), Lateral (LL), and Posterior (LP); and Right Central (RC), Anterior (RA), Lateral (RL), and Posterior (RP) regions. Mid-line sensors appear empty. Lines depict the region boundaries.

et al. (2011). The artefact-removed MEG signals were the input for both approaches used in the inter-regional connectivity assessment. For the sake of illustration, an MEG epoch recorded in the right posterior scalp region after the removal of the cardiac artefact is shown in Fig. 1 for a control, MCI and AD subject.

3. Methods

3.1. Overview

MEG recordings are composed of numerous channels and it may be helpful to group them into regions (Alonso et al., 2011; Poza et al., 2008; Stam et al., 2006). In this study, the channels are grouped into Left Central (LC), Anterior (LA), Lateral (LL), and Posterior (LP); and Right Central (RC), Anterior (RA), Lateral (RL), and Posterior (RP) regions as shown in Fig. 2. This distribution is similar to that by Alonso et al. (2011) and Poza et al. (2008), but it also considers the difference between left and right channels. Mid-line sensors are not considered (Stam et al., 2006).

$c(f)$ is computed with two different approaches. The first one consists of calculating $c(f)$ for all pairs of channels (Stam et al., 2006), resulting in a large number of pair-wise values. Then, the results are averaged considering the region to which

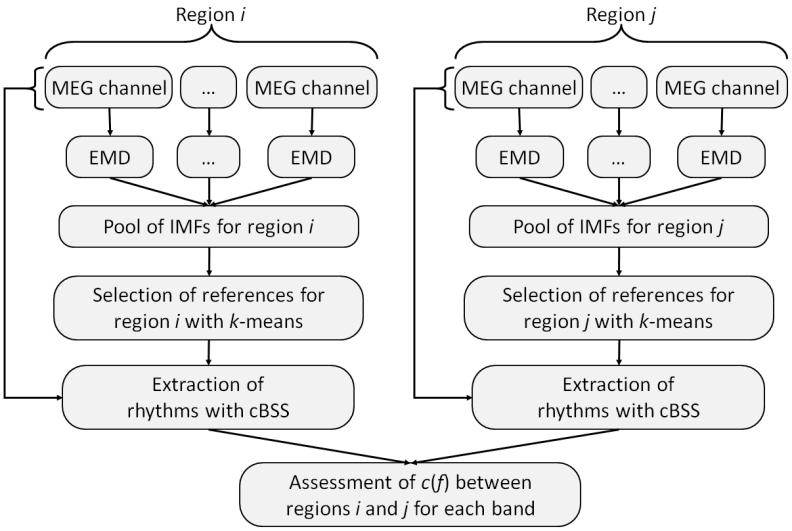

Figure 3: Block diagram of the processing steps included in the second approach to adaptively extract brain activity from each region and compute the $c(f)$ values.

each channel belongs (see Fig. 2) to estimate the inter-regional $c(f)$ in δ (1–4 Hz), θ (4–8 Hz), α (8–13 Hz), and β (13–30 Hz) bands.

In the second approach, the MEG inter-regional $c(f)$ is assessed by means of a novel adaptive procedure to characterise each region and band with a single signal. This approach is illustrated in Fig. 3, where the MEG channels appear on top of the diagram. An EMD is applied to each single channel to obtain the Intrinsic Mode Functions (IMFs) (Huang et al., 1998). Afterwards, all IMFs from channels in the same scalp region are combined into a "pool" of single-channel rhythms. Subsequently, a k-means clustering (Hartigan and Wong, 1979) is used to automatically select reference signals representative of the δ, θ, α, and β bands from the pool of IMFs. Then, these references guide a cBSS (Lu and Rajapakse, 2005) to extract one activity signal that simultaneously characterises all channels in the region for every band. Finally, $c(f)$ is calculated between extracted signals of different regions to assess the connectivity.

3.2. Magnitude Squared Coherence – $c(f)$

$c(f)$ is used to measure brain synchrony (Dauwels et al., 2010; Pereda et al., 2005). It quantifies linear correlations as a function of frequency. $c(f)$ is bounded between 0 and 1. This measure can detect the linear synchronisation between two signals, but it does not discriminate the directionality of the coupling (Dauwels et al., 2010; Pereda et al., 2005; Supp et al., 2007). EEG experiments suggest that $c(f)$ is strongly correlated with other commonly used synchronisation measures (Dauwels et al., 2010).

First of all, two time series of equal length – $x\,(t)$ and $y\,(t)$ – are divided into B equal blocks of 1 s each with 50% overlap. This block length was selected on the basis of the analyses by Dauwels et al. (2010) to estimate the optimum parameters for a $c(f)$ computation similar to our first approach. $c(f)$ is calculated as (Alonso et al.,

2011; Dauwels et al., 2010):

$$c(f) = \frac{|\langle X(f) Y^*(f)\rangle|^2}{|\langle X(f)\rangle|\,|\langle Y(f)\rangle|}, \tag{1}$$

where $X(f)$ and $Y(f)$ are the Fourier transform of $x(t)$ and $y(t)$, respectively, and * is the symbol for complex conjugate. Here, $|\cdot|$ denotes magnitude and $\langle\cdot\rangle$ indicates average over the B blocks (Alonso et al., 2011; Dauwels et al., 2010).

3.3. Adaptive extraction

This subsection describes a novel methodology to adaptively extract the brain activity from subsets of channels. This procedure is illustrated in Fig. 3 and applied to the regions depicted in Fig. 2. It relies on data-driven signal processing techniques such as EMD (Huang et al., 1998), cBSS (Lu and Rajapakse, 2005) and, to a lesser degree, k-means clustering (Hartigan and Wong, 1979). This techniques are represented in the second, fifth and fourth rows of the diagram in Fig. 3, respectively.

3.3.1. Empirical Mode Decomposition. The EMD (Huang et al., 1998) is a technique to adaptively represent non-stationary complex signals as a sum of their oscillations (i.e., IMFs). The EMD considers the oscillations in signals so that each IMF satisfies two basic conditions (Huang et al., 1998):

- In each IMF time series, the number of extrema and the number of zero crossings must be the same or differ, at most, by one.
- At any point, the mean value of the two envelopes defined by the local maxima and minima is zero.

Hence, the IMFs of a unidimensional signal $x(t)$ are calculated as follows (Flandrin et al., 2004):

(i) Set $g_p(t) = x(t)$, with p the index of the extraction.

(ii) Detect the extrema (both maxima and minima) of $g_p(t)$.

(iii) Generate the upper and lower envelopes, $e_u(t)$ and $e_l(t)$ respectively, by connecting the maxima and minima separately with cubic spline interpolations.

(iv) The local mean, $m(t)$, is determined as: $m(t) = [e_u(t) + e_l(t)]/2$.

(v) The IMF should have zero local mean. Thus, subtract $m(t)$ from the signal: $g_p(t) \leftarrow [g_p(t) - m(t)]$.

(vi) Decide whether $g_p(t)$ is already an IMF by checking the two basic conditions described above. Otherwise, repeat steps 2 to 6.

When the first IMF is derived ($p = 1$), set $d_p(t) = g_p(t)$, which is the smallest temporal scale (highest frequencies) in $x(t)$ (Flandrin et al., 2004). In order to find the remaining IMFs, generate the residue $r_p(t)$ of the data by subtracting $d_p(t)$ from the signal as: $r_p(t) = [x(t) - d_p(t)]$ (Flandrin et al., 2004). Then, $r_p(t)$ is considered as the new data and subjected to the same sifting process described above (Flandrin et al., 2004). The sifting process is continued until the final residue is a constant, a monotonic function or a function with one maxima and one minima from which no more IMFs can be derived (Flandrin et al., 2004; Rilling et al., 2003).

After the EMD, the uni-dimensional signal $x(t)$ is represented as:

$$x(t) = \sum_{p=1}^{M} d_p(t) + r_M(t), \tag{2}$$

where M is the number of IMFs and $r_M(t)$ is the final residue (Huang et al., 1998).

3.3.2. Frequency Characterisation of the IMFs. The EMD is applied to each single channel, as represented on top of Fig. 3, to isolate its oscillations. Then, the spectral content of each IMF has to be characterised. In order to do so, the instantaneous frequency of each IMF, $\omega_p(t)$, is computed as (Huang et al., 1998):

$$\omega_p(t) = \frac{d\theta_p(t)}{dt}, \tag{3}$$

where $\theta_p(t)$ denotes the phase of the analytic signal, $z_p(t) = a_p(t)\exp[i\theta_p(t)] = d_p(t) + i\mathcal{H}[d_p(t)]$, computed from each IMF by means of Hilbert transform, $\mathcal{H}[\cdot]$ (Huang et al., 1998).

Afterwards, a weighted average of the instantaneous frequency, $\overline{\omega}_p$, is computed from each $\omega_p(t)$ considering the amplitude:

$$\overline{\omega}_p = \frac{E\{a_p(t)\,\omega_p(t)\}}{E\{a_p(t)\}}, \tag{4}$$

where $E\{\cdot\}$ refers to expectation. $\overline{\omega}_p$ contains the typical frequency of each IMF. Therefore, it characterises its spectral content.

3.3.3. Reference Selection. The IMFs represent oscillations in a single channel but they do not account for the rhythmic activity of a whole region. Therefore, a cBSS (Huang and Mi, 2007; Lu and Rajapakse, 2005) is used to extract the brain activity corresponding to a particular subset of channels for a specific frequency band (δ, θ, α and β). The cBSS needs a suitable reference (Huang and Mi, 2007; James and Gibson, 2003). This reference was selected with a k-means clustering.

The k-means algorithm is an effective and simple clustering procedure and it is appealing for its adaptive nature (Hartigan and Wong, 1979). The algorithm divides a set of features (the $\overline{\omega}_p$ values) into k clusters automatically without any supervision (Hartigan and Wong, 1979). After the initialisation, the k-means clustering assigns the data values to the closest cluster centre. Then, the geometric centre of each cluster is recomputed, meaning that the clusters are re-calculated. These steps are repeated until convergence is reached (Hartigan and Wong, 1979).

For each region, all IMFs whose $\overline{\omega}_p$ value belongs to the broadband of interest (1–30 Hz) are aggregated into a "pool" (see third row of Fig. 3). Then, these $\overline{\omega}_p$ are fed into a k-means clustering initialised with four centroids in the middle of the spectral bands. Once convergence has been reached, the IMF corresponding with the closest $\overline{\omega}_p$ to each cluster's centroid is chosen as the reference for the cBSS applied to the channels from that region. This process is shown in the fourth row of Fig. 3.

3.3.4. Regional Extraction of Brain Activity With cBSS. A reference per region and band is selected with k-means for being representative of the spectral location of the δ, θ, α or β band. Yet, this reference is indeed an IMF, which has been isolated from a single MEG channel. Hence, it is only representative of that channel. This reference will guide a cBSS to extract common activity representatitive for the whole region.

In general, BSS techniques estimate a set of n underlying unknown components – $\mathbf{s}(t) = [s_1(t), \ldots, s_n(t)]^T$ – and the mixing matrix – $\mathbf{A}$ – that generated a set of n observed recordings – $\mathbf{x}(t) = [x_1(t), \ldots, x_n(t)]^T$ – through:

$$\mathbf{x}(t) = \mathbf{A}\mathbf{s}(t). \tag{5}$$

The basic assumption in BSS is that the sources, also known as components, are statistically independent (Escudero et al., 2009; James and Hesse, 2005). An additive noise term can be included in the model to account for the lack of fit. The cBSS methods incorporate additional information into the separations so that the extracted component bears some relationship to a given reference (James and Hesse, 2005).

Diverse implementations of the cBSS have been proposed (Huang and Mi, 2007; Lu and Rajapakse, 2005). Usually, the cBSS introduces a regularisation parameter into a general-purpose BSS algorithm (Huang and Mi, 2007; Lu and Rajapakse, 2005). In this way, the cBSS obtains the statistically independent component that is closest to the reference (James and Gibson, 2003). This reference only needs to be similar enough to drive the cBSS towards the desired component (James and Gibson, 2003).

In this study, the algorithm by Huang and Mi (2007), which improves the method by Lu and Rajapakse (2005), has been used. The reference for the cBSS is the sign function of the IMF selected by the clustering (Huang and Mi, 2007; James and Gibson, 2003). The sign function was applied because the reference signal for the cBSS is most often constructed as a set of on/off pulses that guide the extraction of the components of interest (Huang and Mi, 2007; James and Gibson, 2003; James and Hesse, 2005; Lu and Rajapakse, 2005). Finally, once the brain activity is extracted for each band and region, $c(f)$ is computed. This procedure is illustrated in Fig. 3 by the presentation to the block that computes $c(f)$ of the activities extracted for two different regions.

4. Results

4.1. Overview

After reducing the cardiac artefact, brain connectivity was computed with two different approaches. In the first one, $c(f)$ was calculated for all pairs of channels and the results are averaged accordingly to pairs of regions (Stam et al., 2006). The second approach relied on the steps shown in Fig. 3. Illustrative examples of the outputs at key stages of this approach are given in the following lines.

First of all, an EMD is applied to each single MEG channel to estimate its oscillatory patterns. Fig. 4 depicts the IMFs calculated from the control subject's MEG epoch plotted in Fig. 1. It can be seen that spectral content of the rhythms moves from fast to slow frequencies as more IMFs are computed.

Secondly, each IMF is characterised with its $\overline{\omega}_p$ and a pool of IMFs from the same region is created. Then, k-means is applied to find the IMFs whose $\overline{\omega}_p$ values are the most representative (i.e., central) of the δ, θ, α, and β bands. This process is exemplified in Fig. 5 for the IMFs of the same subject and region as Fig. 4. Fig. 5 indicates the number of IMFs that have a particular value of $\overline{\omega}_p$ in the y axis. The vertical lines represent the centroid of each cluster.

Finally, once the reference for each region and band has been selected, the cBSS extracted the dominant activity in the band of interest for the region under consideration. All MEG channels from a region, together with the reference IMF selected by k-means, are fed to the cBSS. Then, the cBSS extracts a component that

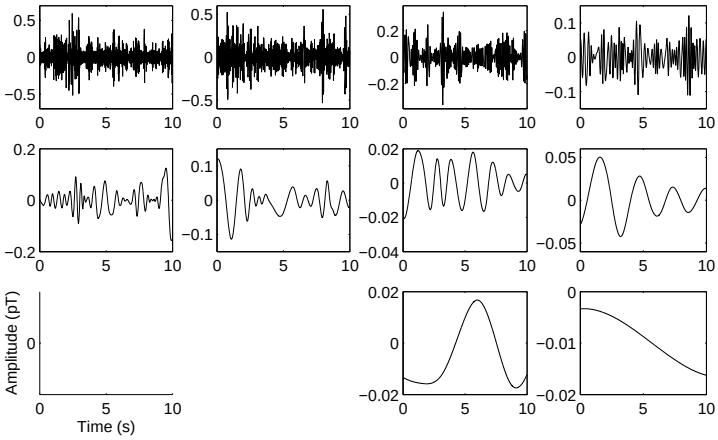

Figure 4: IMFs obtained from the control subject's MEG channel depicted in Fig. 1 plotted following their order of extraction from left to right and top to bottom.

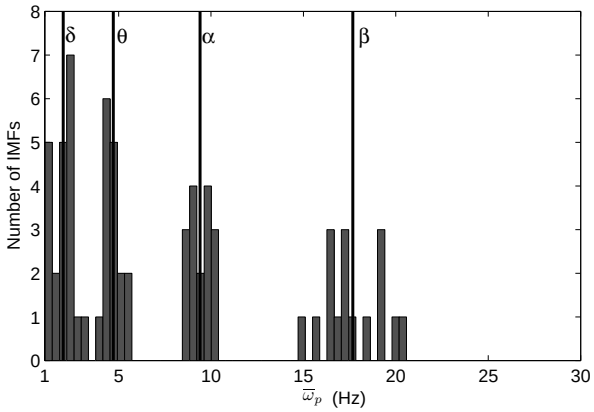

Figure 5: Reference selection with k-means applied to RP region in the same control subject's MEG epoch as in Fig. 1. The four vertical lines indicate the position of the centroids for δ, θ, α and β.

is statistically independent from the rest of the activity and similar to the reference. This computation is represented in Fig. 6 for the α band of the same subject and region as in Fig. 5.

In both approaches, the results were averaged for all MEG epochs so that the value of $c(f)$ per band, pair of regions, and subject was obtained. It must be noticed that the $c(f)$ values correspond to inter-regional, probably long-distance, brain connectivity.

4.2. Descriptive Statistical Analysis

Qualitative statistical analysis was performed to gain insight into the $c(f)$ values of AD, MCI and control subjects. Firstly, a repeated-measures ANalysis Of VAriance (ANOVA) was performed with the Greenhouse-Geisser correction for the lack of sphericity. The group (AD vs. MCI vs. controls) was the inter-subject factor while the

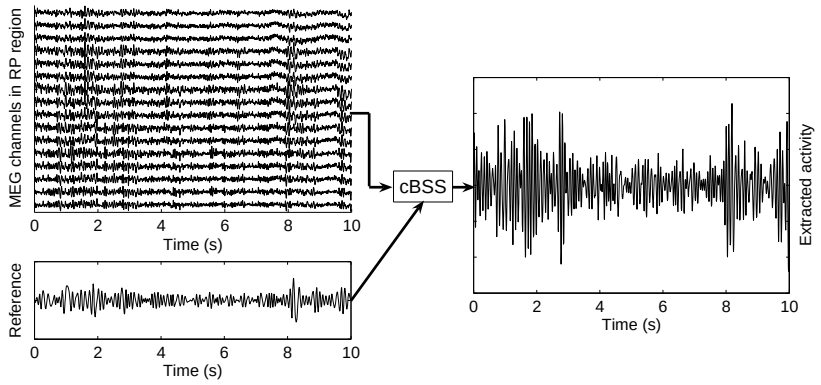

Figure 6: Illustration of the cBSS procedure for α band in the RP region and for the same control subject's MEG epoch as in Fig. 1.

variables 'Band' (δ, θ, α and β) and 'Pair of regions' were taken as intra-subject factors. For the first approach, the ANOVA reported significant effects involving the factors 'Band', 'Pair' and their interaction ($p < 0.0001$). On the other hand, the inter-subject factor ('Diagnosis') was not significant ($p = 0.1015$). In the case of the EMD and cBSS approach, the effects of 'Band' ($p = 0.0132$) 'Pair' and 'Band×Pair' ($p < 0.0001$) were also significant. The effect of 'Diagnosis' was not significant ($p = 0.7005$) when all bands and pairs were simultaneously considered in the ANOVA.

A repeated-measures ANOVA (Greenhouse-Geisser correction) was applied to every band with 'Pair of regions' as the only intra-subject factor. For both approaches and all bands, there was a significant effect due to 'Pair of regions'. The level of $c(f)$ depended on the distance between the regions – e.g., the overall $c(f)$ level between regions located over the same hemisphere was usually higher than for pairs of left and right regions. 'Diagnosis' only had a significant effect for the δ band in the first approach ($p = 0.0100$).

In order to further explore the results, we inspected the estimated marginal means for the three subject groups for each band and approach. Fig. 7 depicts these estimated marginal means, which revealed slight differences in the overall levels of inter-regional $c(f)$ for each approach. The estimated marginal means suggest that AD increases the level of $c(f)$ in the δ band while MCI subjects tends to have lower connectivity in θ. The results in the upper bands are not conclusive, but a slight reduction in α inter-regional connectivity was found with the second approach. In addition, the estimated marginal means of $c(f)$ for the extracted brain activity were consistently lower than those values computed from the MEG channels (first approach).

4.3. Classification Analysis

We also measured the ability of $c(f)$ to distinguish the groups in both approaches. A stepwise logistic regression with a full leave-one-out cross-validation (loo-cv) was applied to the $c(f)$ values from every band to classify the subjects into diagnosis pairs (controls vs. MCI, controls vs. AD, and MCI vs. AD). This procedure used all available subjects but one to develop a classifier which was tested on the left-out subject. Then, this process was repeated for the other subjects. At every iteration, a forward stepwise variable selection was used to decide which variables would be included (if their

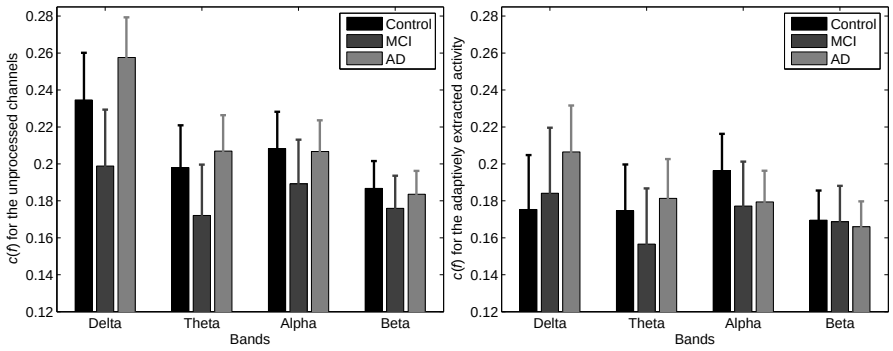

Figure 7: Estimated marginal means, with 95% confidence interval, of $c(f)$ from AD, MCI and control subjects in each spectral band for both approaches: (a) first approach, based on MEG channels, and (b) second approach, when EMD and cBSS were used for activity extraction.

Table 1: Pairwise stepwise logistic regression classification with a full loo-cv for the $c(f)$ computed from the MEG channels. The number of variables that were automatically selected in more than half the number of cases is also shown.

C vs. M					
Band	δ	θ	α	β	Comb.
C correctly classified (%)	57.7	46.2	57.7	50.0	57.7
M correctly classified (%)	61.1	44.4	50.0	77.8	61.1
Global rate (%)	59.1	45.5	54.5	61.4	59.1
Commonly selected variables	1	1	3	1	1
C vs. A					
Band	δ	θ	α	β	Comb.
C correctly classified (%)	42.3	69.2	53.8	42.3	46.2
A correctly classified (%)	36.1	55.6	55.6	44.4	55.6
Global rate (%)	38.7	61.3	54.8	43.5	51.6
Commonly selected variables	0	0	3	2	2
M vs. A					
Band	δ	θ	α	β	Comb.
M correctly classified (%)	55.6	66.7	66.7	38.9	55.6
A correctly classified (%)	63.9	44.4	69.4	72.2	63.9
Global rate (%)	61.1	51.9	68.5	61.1	61.1
Commonly selected variables	1	1	2	0	2

C, M, and A refer to controls, MCI, and AD patients, respectively.
'Comb.' indicates that a combination of features of all bands was entered.

associated $p < 0.05$) or removed (if $p > 0.10$) in the classifier. Table 1 and Table 2 show the classification results based on $c(f)$ from the original MEG channels and from the extracted activity, respectively, as percentage of subjects correctly classified in each case (band and diagnoses).

Table 2: Pairwise stepwise logistic regression classification with a full loo-cv for the $c(f)$ of the adaptively extracted rhythms. The number of variables that were automatically selected in more than half the number of cases is also shown.

C vs. M					
Band	δ	θ	α	β	Comb.
C correctly classified (%)	84.6	73.1	69.2	69.2	73.1
M correctly classified (%)	44.4	66.7	44.4	55.6	83.3
Global rate (%)	68.2	70.5	59.1	63.6	77.3
Commonly selected variables	2	1	1	3	4
C vs. A					
Band	δ	θ	α	β	Comb.
C correctly classified (%)	69.2	50.0	53.8	84.6	84.6
A correctly classified (%)	69.4	47.2	75.0	47.2	58.3
Global rate (%)	69.4	48.4	66.1	62.9	69.4
Commonly selected variables	1	0	3	0	2
M vs. A					
Band	δ	θ	α	β	Comb.
M correctly classified (%)	11.1	55.6	22.2	83.3	72.2
A correctly classified (%)	72.2	47.2	58.3	55.6	63.9
Global rate (%)	51.9	50.0	46.3	64.8	66.7
Commonly selected variables	2	1	0	2	2

C, M, and A refer to controls, MCI, and AD patients, respectively.
'Comb.' indicates that a combination of features of all bands was entered.

Table 1 and Table 2 also display the number of variables that were included in the logistic regression in more than 50% of the iterations for every case. These consistently selected variables of individual bands were combined and the classification process repeated to check whether diverse spectral bands could have complementary information for the detection of MCI and AD. These results appear under the 'Comb.' headers in Table 1 and Table 2.

5. Discussion and Conclusions

MEG background activity from 36 AD, 18 MCI and 26 control subjects was analysed to assess the MEG inter-regional connectivity with $c(f)$. Furthermore, a novel procedure to adaptively extract brain rhythmic activity from sets of channels was proposed. Hence, the aim of this study was twofold: to inspect the alterations that AD and MCI cause in the electromagnetic brain activity and to introduce a methodology based on EMD and cBSS to extract brain activity in δ, θ, α and β bands. The statistical analysis suggested that AD and MCI might affect the inter-regional connectivity, although the results were not statistically significant. However, a logistic regression with full loo-cv indicated that our methodology had higher accuracy in the classification of MCI and AD than computing $c(f)$ from the raw MEGs.

The cardiac contamination was reduced using a cBSS-based scheme (Escudero et al., 2011; James and Gibson, 2003). This ensured that the QRS complexes did not affect the IMFs that could serve as references to extract the rhythmic oscillations. Otherwise, the cardiac activity might have been present in some of the IMFs (Blanco-

Velasco et al., 2008), thus biasing the results. The same cardiac activity was estimated using the cBSS and removed from all MEG channels in order to avoid differences in the way the channels were preprocessed. This artefact removal was applied before any connectivity-related computation. Hence, the differences in the results between both approaches cannot be due to that. Additionally, it is important to note that the MEG may suffer from baseline drifts or high-frequency noise. However, our analysis in the second approach is robust to the presence of these kinds of noise. Firstly, only frequencies between 1–30 Hz were considered in the calculation of $c(f)$. This spectral range includes the δ, θ, α and β bands while discarding the very low-frequency baseline drifts, whose spectrum is located below 1 Hz, and any high-frequency contamination over 30 Hz. Furthermore, the EMD isolates the high-frequency noise and the baseline drift in the first and last extracted IMFs, respectively. Since only the IMFs whose $\overline{\omega}_p$s are between 1–30 Hz are fed to the clustering process, the IMFs that account for baseline drift or high-frequency noise cannot be selected as references for the cBSS. Actually, the ability of the EMD to isolate baseline wanders and noise has been used to denoise biomedical recordings (Blanco-Velasco et al., 2008).

Suitable references were selected among all IMFs from a region for each band. This procedure was carried out using a k-means clustering of the $\overline{\omega}_p$ values. Then, a cBSS was applied to simultaneously extract the activities from all channels in a region. This allowed us to consider the activity at the regional level, which is in contrast with processing single channels – 'channel domain', (Alonso et al., 2011; Gómez et al., 2009b) – or localising equivalent dipoles – 'dipole domain', (Hoechstetter et al., 2004; Rossini et al., 2007; Supp et al., 2007). Our approach is slightly similar to that adopted by Stam et al. (2006), who carried out a channel-wise analysis and then grouped and averaged the results. Alternatively, we took a 'regional domain' approach and tested it on the classification of MCI and AD subjects. AD causes a slowdown and abnormalities in the non-linear dynamics of the electromagnetic brain activity (Hornero et al., 2009; Jeong, 2004; Rossini et al., 2007; Stam, 2010). Although AD has been related to neo-cortical disconnection (Jeong, 2004), this effect is not always easily detectable (Dauwels et al., 2010). There is some consensus that AD decreases the synchronisation level in high-frequency bands. Contradictory results have been found for low frequencies (Jeong, 2004; Rossini et al., 2007), but animal models suggest that acetylcholine loss decreases high-frequency EEG connectivity while increasing low-frequency coupling (Rossini et al., 2007).

Although $c(f)$ only captures linear signal interactions (Gómez et al., 2009b; Pereda et al., 2005), it is not clear whether the alternative non-linear connectivity measures are superior to $c(f)$ (Gómez et al., 2009b). Moreover, the outcomes of $c(f)$ and other connectivity measurements seem to be correlated (Dauwels et al., 2010). Diverse EEG studies have applied $c(f)$ to study MCI patients (Babiloni et al., 2006; Dauwels et al., 2010; Jeong, 2004; Rossini et al., 2006, 2007). It has been suggested that $c(f)$ might help to estimate the progression from MCI to AD (Rossini et al., 2006). Yet, there are some divergences among studies, which might be due to differences in the analysed populations and the heterogeneity of MCI (Gómez et al., 2009b).

The statistical analysis showed clear dependences of $c(f)$ on the spectral band and pair of regions. The estimated marginal means supported the idea that AD decreases the connectivity of brain signals in α (Jeong, 2004; Rossini et al., 2007; Stam, 2010). Moreover, they seemed to suggest that AD causes a rise in δ $c(f)$ levels. However, there were no significant differences between the groups. The fact that not all frequencies are equally affected by the changes in $c(f)$ indicates that the alterations

are not simply due to a loss of cortical neurons (Dauwels et al., 2010). Moreover, previous studies have reported opposite changes in different spectral bands in relation to AD (Alonso et al., 2011; Stam et al., 2009; van Cappellen van Walsum et al., 2003). Actually, our results complement the intra-regional connectivity analysis by Alonso et al. (2011), who reported an intra-regional increase in connectivity in low frequencies and a decrease in fast rhythms in a smaller sample of AD patients. The alterations in connectivity might be due to anatomical disconnections among cortical regions or reduced cholinergic coupling between cortical neurons (Dauwels et al., 2010).

A stepwise procedure automatically selected the most appropriate features from each single spectral band to classify the subjects at every single iteration of the loo-cv. This ensured that the development of the classifier (i.e., variable selection and training of the logistic regression) was not influenced at all by the testing data. We also evaluated the possible complementarity of features from diverse bands to diagnose the subjects. In these cases, only variables that had been frequently selected in single bands were presented to the classifier development. The aim was to avoid the over-fitting that would have appeared if all features from all bands (112 variables in total) had been used to classify a few dozens of subjects. The loo-cv reduces the accuracy levels but it avoids over-estimation of the true classification rates and increases the reproducibility of the results (Dauwels et al., 2010). It must be noted that the number of variables selected by the stepwise procedure (with a maximum of 4) was small in comparison with the total number of features available for classification. Moreover, the combination of features from several bands tended to improve the performance of the classifier based on the $c(f)$ calculated with the proposed methodology.

Reported MEG-based classification rates of AD patients versus healthy elderly subjects usually are about 80% (Escudero et al., 2009; Gómez et al., 2009a; Hornero et al., 2009; Poza et al., 2008; Stam, 2010). Our highest accuracies are relatively lower than those, but comparable to those found by Alonso et al. (2011) in a smaller dataset. However, cross-validation techniques were not always applied in other papers. In this study, the accuracy reached 69.4% when variables of all bands were combined in the second approach to separate AD patients from controls.

The use of $c(f)$ features allowed us to classify MCI and control subjects with an accuracy of 77.3%. This value is lower than the accuracy obtained in an EEG study with neural networks (93.5%) (Rossini et al., 2008) but close to that recently reported after an exhaustive EEG connectivity analysis (83%) (Dauwels et al., 2010). However, care should be taken when comparing these results as different types of signals were studied. A difference of more than 12 years in the mean age of MCI and controls existed in the work by Rossini et al. (2008) while the groups were matched in age in our study. Furthermore, our result compares favourably with a previous study that classified a similar dataset of MCI and controls with accuracy of 69.8% without cross-validation (Gómez et al., 2009b).

Rather than trying to estimate the equivalent current dipoles or computing $c(f)$ for pairs of channels, the activity was extracted at a regional level. It is important to note that the cBSS does not estimate equivalent current dipoles. Instead, it extracts a signal component that is independent from the rest of the brain activity and close to a reference (Huang and Mi, 2007; James and Gibson, 2003; Lu and Rajapakse, 2005). This procedure allowed us to obtain the activity that jointly represents a set of channels (Lu and Rajapakse, 2005). Thus, the extracted component accounts for the dominant activity in each of the bands of interest for every region. This novel approach led to two noticeable results. Firstly, the estimated marginal means tended to be lower when

$c(f)$ was computed with the proposed methodology than when calculated from the raw MEG channels. Secondly, the adaptive extraction of activity used to provide higher classification accuracies than the MEG channels. A potential explanation for these two results might be that the extraction helped to reduce the impact of the contamination from other activities into the inter-regional connectivity. This might alleviate the volume conduction effect, which is stronger at nearby channels, and its associated bias in $c(f)$ (Nolte et al., 2004; Stam et al., 2009). Nevertheless, we do acknowledge that additional tests are needed to corroborate or refute this hypothetical explanation. Other limitations of this study also merit consideration. Firstly, the sample size is small to prove the usefulness of our approach as a diagnostic tool. Thus, a larger database is needed to confirm the results. Secondly, and similarly to other studies (Dauwels et al., 2010), we mainly tried to help in the discrimination of subject groups. We did not aim at identifying the biophysical mechanisms that cause the alterations of AD and MCI in the MEGs. Finally, the subjects did not perform any specific task. Hence, the classification performance might be improved by analysing signals acquired during specific tasks (Dauwels et al., 2010; Stam, 2010).

To sum up, we have introduced a novel methodology to extract the activity from MEG scalp regions. We have also assessed the connectivity alterations caused by AD and MCI in the electromagnetic brain activity. Our results suggest that the proposed methodology could provide information about the connectivity pattern in MEG. Furthermore, they prove the usefulness of this procedure in the classification of AD and MCI patients versus healthy elderly subjects.

Acknowledgments

The authors would like to thank the "Asociación de Familiares de Enfermos de Alzheimer" (Madrid, Spain) for providing the patients who participated in this study and Dr. Alberto Fernández ("Centro de Magnetoencefalografía Dr. Pérez-Modrego"), who collected the MEG recordings. They are also thankful to the Reviewers and the Editorial Office for their feedback about the manuscript.

This work was supported in part by the Spanish "Ministerio de Ciencia e Innovación" (Ref: TEC2008-02241) and by a Spanish FPU grant (Ref: AP2007-03303) awarded to J. Escudero.

References

D. Abásolo, J. Escudero, R. Hornero, C. Gómez, and P. Espino. Approximate entropy and auto mutual information analysis of the electroencephalogram in Alzheimer's disease patients. *Medical and Biological Engineering and Computing*, 46(10):1019–1028, 2008.

I. Abatzoglou, P. Anninos, A. Adamopoulos, and M. Koukourakis. Nonlinear analysis of brain magnetoencephalographic activity in Alzheimer disease patients. *Acta Neurologica Belgica*, 107(2):34–39, 2007.

I. Abatzoglou, P. Anninos, I. Tsalafoutas, and M. Koukourakis. Multi-channel magnetoencephalogram on Alzheimer disease patients. *Journal of integrative neuroscience*, 8(1):13–22, 2009.

J. Alonso, J. Poza, M. Mañanas, S. Romero, A. Fernández, and R. Hornero. MEG connectivity analysis in patients with Alzheimer's disease using cross mutual

information and spectral coherence. *Annals of Biomedical Engineering*, 39(1):524–536, 2011.

C. Babiloni, R. Ferri, G. Binetti, A. Cassarino, G. D. Forno, M. Ercolani, F. Ferreri, G. B. Frisoni, B. Lanuzza, C. Miniussi, F. Nobili, G. Rodriguez, F. Rundo, C. J. Stam, T. Musha, F. Vecchio, and P. M. Rossini. Fronto-parietal coupling of brain rhythms in mild cognitive impairment: A multicentric EEG study. *Brain Research Bulletin*, 69(1):63–73, 2006.

M. Blanco-Velasco, B. Weng, and K. Barner. ECG signal denoising and baseline wander correction based on the empirical mode decomposition. *Computers in Biology and Medicine*, 38(1):1–13, Jan. 2008.

K. Blennow, de Leon M.J., and H. Zetterberg. Alzheimer's disease. *The Lancet*, 368 (9533):387–403, 2006.

J. Dammers, M. Schiek, F. Boers, C. Silex, M. Zvyagintsev, U. Pietrzyk, and K. Mathiak. Integration of amplitude and phase statistics for complete artifact removal in independent components of neuromagnetic recordings. *IEEE Transactions on Biomedical Engineering*, 55(10):2353–2362, 2008.

J. Dauwels, F. Vialatte, T. Musha, and A. Cichocki. A comparative study of synchrony measures for the early diagnosis of Alzheimer's disease based on EEG. *NeuroImage*, 49(1):668–693, Jan. 2010.

J. Escudero, R. Hornero, D. Abásolo, A. Fernández, and M. López-Coronado. Artifact removal in magnetoencephalogram background activity with independent component analysis. *IEEE Transactions on Biomedical Engineering*, 54(11):1965–1973, Nov. 2007.

J. Escudero, R. Hornero, D. Abásolo, and A. Fernández. Blind source separation to enhance spectral and non-linear features of magnetoencephalogram recordings. Application to Alzheimer's disease. *Medical Engineering and Physics*, 31(7):872–879, 2009.

J. Escudero, R. Hornero, D. Abásolo, and A. Fernández. Quantitative Evaluation of Artifact Removal in Real Magnetoencephalogram Signals With Blind Source Separation. *Annals of Biomedical Engineering*, In press(DOI: 10.1007/s10439-011-0312-7), 2011.

A. Fernández, R. Hornero, A. Mayo, J. Poza, P. Gil-Gregorio, and T. Ortiz. MEG spectral profile in Alzheimer's disease and mild cognitive impairment. *Clinical Neurophysiology*, 117(2):306–314, 2006.

C. P. Ferri, M. Prince, C. Brayne, H. Brodaty, L. Fratiglioni, M. Ganguli, K. Hall, K. Hasegawa, H. Hendrie, Y. Huang, A. Jorm, C. Mathers, P. R. Menezes, E. Rimmer, and M. Scazufca. Global prevalence of dementia: a Delphi consensus study. *The Lancet*, 366(9503):2112–2117, 2006.

P. Flandrin, G. Rilling, and P. Gonçalvès. Empirical mode decomposition as a filter bank. *IEEE Signal Processing Letters*, 11(2):112–114, Feb. 2004.

M. Folstein, S. Folstein, and P. McHugh. Mini-mental state. A practical method for grading the cognitive state of patients for the clinician. *Journal of Psychiatric Research*, 12(3):189–198, Nov. 1975.

C. Gómez, R. Hornero, D. Abásolo, A. Fernández, and J. Escudero. Analysis of MEG background activity in Alzheimer's disease using nonlinear methods and ANFIS. *Annals of Biomedical Engineering*, 37(3):586–594, 2009a.

C. Gómez, C. Stam, R. Hornero, A. Fernández, and F. Maestú. Disturbed beta band functional connectivity in patients with mild cognitive impairment: An MEG study. *IEEE Transactions on Biomedical Engineering*, 56(6):1683–1690, Jun. 2009b.

J. Hartigan and M. Wong. A k-means clustering algorithm. *Journal of the Royal Statistical Society. Series C (Applied Statistics)*, 28(1):100–108, 1979.

K. Hoechstetter, H. Bornfleth, D. Weckesser, N. Ille, P. Berg, and M. Scherg. BESA source coherence: a new method to study cortical oscillatory coupling. *Brain topography*, 16(4):233–238, 2004.

R. Hornero, J. Escudero, A. Fernández, J. Poza, and C. Gómez. Spectral and nonlinear analyses of MEG background activity in patients with Alzheimer's disease. *IEEE Transactions on Biomedical Engineering*, 55(6):1658–1665, 2008.

R. Hornero, D. Abásolo, J. Escudero, and C. Gómez. Nonlinear analysis of electroencephalogram and magnetoencephalogram recordings in patients with Alzheimer's disease. *Philosophical Transactions of the Royal Society A: Mathematical, Physical and Engineering Sciences*, 367(1887):317–336, Jan. 2009.

D. Huang and J. Mi. A new constrained independent component analysis method. *IEEE Transactions on Neural Networks*, 18(5):1532–1535, Sep. 2007.

N. Huang, Z. Shen, S. Long, M. Wu, H. Shih, Q. Zheng, N. Yen, C. Tung, and H. Liu. The empirical mode decomposition and the Hilbert spectrum for nonlinear and non-stationary time series analysis. *Proceedings of the Royal Society of London. Series A: Mathematical, Physical and Engineering Sciences*, 454(1971):903–995, 1998.

C. James and O. Gibson. Temporally constrained ICA: An application to artifact rejection in electromagnetic brain signal analysis. *IEEE Transactions on Biomedical Engineering*, 50(9):1108–1116, Sep. 2003.

C. James and C. Hesse. Independent component analysis for biomedical signals. *Physiological Measurement*, 26(1):R15–R39, Feb. 2005.

J. Jeong. EEG dynamics in patients with Alzheimer's disease. *Clinical Neurophysiology*, 115(7):1490–1505, Jul. 2004.

W. Lu and J. Rajapakse. Approach and applications of constrained ICA. *IEEE Transactions on Neural Networks*, 16(1):203–212, Jan. 2005.

G. McKhann, D. Drachman, M. Folstein, R. Katzman, D. Price, and E. Stadlan. Clinical diagnosis of Alzheimer's disease: Report of the NINCDS-ADRDA Work Group under the auspices of Department of Health and Human Services Task Force on Alzheimer's Disease. *Neurology*, 34(7):939–944, 1984.

P. Nestor, P. Scheltens, and J. Hodges. Advances in the early detection of Alzheimer's disease. *Nature Reviews Neuroscience*, 5(Supplement):S34–S41, 2004.

G. Nolte, O. Bai, L. Wheaton, Z. Mari, S. Vorbach, and M. Hallett. Identifying true brain interaction from EEG data using the imaginary part of coherency. *Clinical Neurophysiology*, 115(10):2292–2307, 2004.

E. Pereda, R. Quiroga, and J. Bhattacharya. Nonlinear multivariate analysis of neurophysiological signals. *Progress in Neurobiology*, 77(1–2):1–37, Sep.-Oct. 2005.

R. Petersen, J. Stevens, M. Ganguli, E. Tangalos, J. Cummings, and S. DeKosky. Practice parameter: Early detection of dementia: Mild cognitive impairment (an evidence-based review): Report of the Quality Standards Subcommittee of the American Academy of Neurology. *Neurology*, 56(9):1133–1142, 2001.

J. Poza, R. Hornero, J. Escudero, A. Fernández, and C. Sánchez. Regional Analysis of Spontaneous MEG Rhythms in Patients with Alzheimer's Disease Using Spectral Entropies. *Annals of Biomedical Engineering*, 36(1):141–152, Jan. 2008.

B. Reisberg. Functional assessment staging (FAST). *Psychopharmacology Bulletin*, 24(4):653–659, 1988.

G. Rilling, P. Flandrin, and P. Gonçalvès. On empirical mode decomposition and its algorithms. In *IEEE EURASIP Workshop on Nonlinear Signal and Image Processing NSIP-03, Grado, Italy*, 2003.

P. Rossini, C. D. Percio, P. Pasqualetti, E. Cassetta, G. Binetti, G. D. Forno, F. Ferreri, G. Frisoni, P. Chiovenda, C. Miniussi, L. Parisi, M. Tombini, F. Vecchio, and C. Babiloni. Conversion from mild cognitive impairment to Alzheimer's disease is predicted by sources and coherence of brain electroencephalography rhythms. *Neuroscience*, 143(3):793–803, 2006.

P. Rossini, S. Rossi, C. Babiloni, and J. Polich. Clinical neurophysiology of aging brain: from normal aging to neurodegeneration. *Progress in Neurobiology*, 83(6): 375–400, Dec. 2007.

P. Rossini, M. Buscema, M. Capriotti, E. Grossi, G. Rodriguez, C. Del Percio, and C. Babiloni. Is it possible to automatically distinguish resting EEG data of normal elderly vs. mild cognitive impairment subjects with high degree of accuracy? *Clinical Neurophysiology*, 119(7):1534–1545, 2008.

T. Sander, M. Burghoff, P. Van Leeuwen, and L. Trahms. Application of decorrelation-independent component analysis to biomagnetic multi-channel measurements. *Biomedizinische Technik*, 52(1):130–136, 2007.

C. Stam. Use of magnetoencephalography (MEG) to study functional brain networks in neurodegenerative disorders. *Journal of the Neurological Sciences*, 289(1–2):128–134, Feb. 2010.

C. Stam, B. Jones, I. Manshanden, A. van Cappellen van Walsum, T. Montez, J. Verbunt, J. de Munck, B. van Dijk, H. Berendse, and P. Scheltens. Magnetoencephalographic evaluation of resting-state functional connectivity in Alzheimer's disease. *NeuroImage*, 32(3):1335–1344, Sep. 2006.

C. Stam, W. De Haan, A. Daffertshofer, B. Jones, I. Manshanden, A. Van Cappellen van Walsum, T. Montez, J. Verbunt, J. De Munck, B. Van Dijk, H. Berendse, and P. Scheltens. Graph theoretical analysis of magnetoencephalographic functional connectivity in Alzheimer's disease. *Brain*, 132(1):213–224, 2009.

G. Supp, A. Schlögl, N. Trujillo-Barreto, M. Müller, and T. Gruber. Directed cortical information flow during human object recognition: analyzing induced EEG gamma-band responses in brain's source space. *PLoS One*, 2(8):e684, 2007.

A. van Cappellen van Walsum, Y. Pijnenburg, H. Berendse, B. van Dijk, D. Knol, P. Scheltens, and C. Stam. A neural complexity measure applied to MEG data in Alzheimer's disease. *Clinical Neurophysiology*, 114(6):1034–1040, 2003.

Y. Ye-Lin, J. Garcia-Casado, G. Prats-Boluda, and J. Martinez-de Juan. Combined method for reduction of high frequency interferences in surface electroenterogram (EEnG). *Annals of Biomedical Engineering*, 38(7):2358–2370, Jul. 2010.